

A Short-Pulse Area MTI

Ben H. CANTRELL

*Radar Analysis Staff
Radar Division*

September 22, 1977

PLEASE RETURN THIS COPY TO:

NAVAL RESEARCH LABORATORY

WASHINGTON, D.C. 20375

ATTN: CODE 2628

Because of our limited supply you are requested to return this copy as soon as it has served your purposes so that it may be made available to others for reference use. Your cooperation will be appreciated.

NDW-NRL-5070/2616 (1-84)

NAVAL RESEARCH LABORATORY

Washington, D.C.

REPORT DOCUMENTATION PAGE		READ INSTRUCTIONS BEFORE COMPLETING FORM
1. REPORT NUMBER NRL Report 8162	2. GOVT ACCESSION NO.	3. RECIPIENT'S CATALOG NUMBER
4. TITLE (and Subtitle) A SHORT-PULSE AREA MTI	5. TYPE OF REPORT & PERIOD COVERED Interim report on a continuing NRL Problem	
7. AUTHOR(s) Ben H. Cantrell	6. PERFORMING ORG. REPORT NUMBER	
9. PERFORMING ORGANIZATION NAME AND ADDRESS Naval Research Laboratory Washington, D.C. 20375	8. CONTRACT OR GRANT NUMBER(s)	
11. CONTROLLING OFFICE NAME AND ADDRESS Department of the Navy Office of Naval Research Arlington, VA 22217	10. PROGRAM ELEMENT, PROJECT, TASK AREA & WORK UNIT NUMBERS NRL Problem R02-97 Project RR021-05-41 Program Element 61153N-21	
14. MONITORING AGENCY NAME & ADDRESS (if different from Controlling Office)	12. REPORT DATE September 22, 1977	
	13. NUMBER OF PAGES 11	
	15. SECURITY CLASS. (of this report) Unclassified	
	15a. DECLASSIFICATION/DOWNGRADING SCHEDULE	
16. DISTRIBUTION STATEMENT (of this Report) Approved for public release; distribution unlimited		
17. DISTRIBUTION STATEMENT (of the abstract entered in Block 20, if different from Report)		
18. SUPPLEMENTARY NOTES		
19. KEY WORDS (Continue on reverse side if necessary and identify by block number) MTI Signal processing Detection		
20. ABSTRACT (Continue on reverse side if necessary and identify by block number) Slow-moving and fast-moving objects can be discriminated between by noncoherently subtracting the video return of a pulse of a short-pulse radar from the video return of the preceding pulse. Under the condition of the scattering object acting as a point target, the probability of detection versus object speed for various signal-to-noise ratios and a fixed probability of false alarm was found. The results showed low detectability for slow-speed targets and high detectability for higher speed targets. The velocity range of low detectability was a function of signal-to-noise ratio. This moving-target detector		

(Continued)

20. ABSTRACT (Continued)

does not have velocity or range ambiguities, as often is the case with moving-target detectors based on doppler processing.

CONTENTS

INTRODUCTION	1
GENERAL OPERATION	1
NOISE CHARACTERISTICS AND THRESHOLDS	2
SIGNAL-PLUS-NOISE CHARACTERISTICS	4
OPERATING CURVES	6
SUMMARY	8



A SHORT-PULSE AREA MTI

INTRODUCTION

Most radars in the past have used doppler information to discriminate between moving and nonmoving targets. Systems using the doppler principle such as systems using a moving-target indicator (MTI), pulse doppler, phase progression on long codes, and modulated CW have been studied extensively [1,2]. An alternate means of discriminating between moving and nonmoving targets is an area MTI [1]. Early work required storing a complete scan of radar video on a storage tube and subtracting the next scan of video from it. As suggested in a recent patent application [3], this could be done on a pulse-to-pulse basis using much less memory if a short pulse were used. The basic principle is that the video return from objects which do not move will cancel and the video from objects which do move will change range cells between pulses and consequently will not cancel.

This report analyzes a special case of this form of short-pulse MTI. The object is assumed to be a point target moving at a constant speed with no other reflectors in the immediate vicinity. The returned signal is corrupted with thermal noise and processed. The result which will be obtained is the probability of detection versus target speed for various signal-to-noise ratios and a fixed false-alarm rate.

GENERAL OPERATION

A radar transmits two short pulse bursts of RF energy separated in time by T . The radar echoes from a point target corrupted by thermal receiver noise are represented at base-band by

$$x_{I1} = m(t - \tau) (\cos \psi) + n_{I1}$$

and

$$x_{Q1} = m(t - \tau) (\sin \psi) + n_{Q1}$$

for the echo of the first pulse and

$$x_{I2} = m[t - (\tau + 2vT/c)] [\cos(\psi + \omega_d T)] + n_{I2}$$

and

$$x_{Q2} = m[t - (\tau + 2vT/c)] [\sin(\psi + \omega_d T)] + n_{Q2}$$

for the echo of the second pulse, where x_{I1} , x_{Q1} , x_{I2} , and x_{Q2} are the in-phase and quadrature components of the first and second echo signals, $m(\cdot)$ is the pulse envelope, t is time, τ is the transmission delay at the first pulse, ψ is an arbitrary phase, v is the velocity of the point target, c is the speed of light, T is the time between pulses, and $\omega_d T$ is the phase shift of the carrier with respect to the first pulse echo due to the doppler shift in the radian frequency ω_d . The terms n_{I1} , n_{Q1} , n_{I2} , and n_{Q2} are zero-mean Gaussian noise with variances of σ^2 , and they are all assumed to be independent. The pulse envelope $m(t)$ is assumed to be

$$m(t) = A \frac{\sin U}{U} \frac{\pi^2}{\pi^2 - U^2},$$

where $U = 1.44\pi t/\tau_p$, A is the pulse amplitude, and τ_p is the pulse width defined by the 3-dB points. The signal-to-noise ratio S/N is then defined by

$$S/N = A^2/2\sigma^2. \tag{1}$$

The two successive pulse radar echoes are envelope detected, which is described by

$$r_1 = \sqrt{x_{I1}^2 + x_{Q1}^2}$$

and

$$r_2 = \sqrt{x_{I2}^2 + x_{Q2}^2},$$

where r_1 and r_2 are the envelope-detected signals of the first and second pulse respectively. The moving-target detector operates by storing the returned signal as a function of range (or time) from the first pulse and subtracting the return at the corresponding range (or time) of the second pulse. This operation is given by

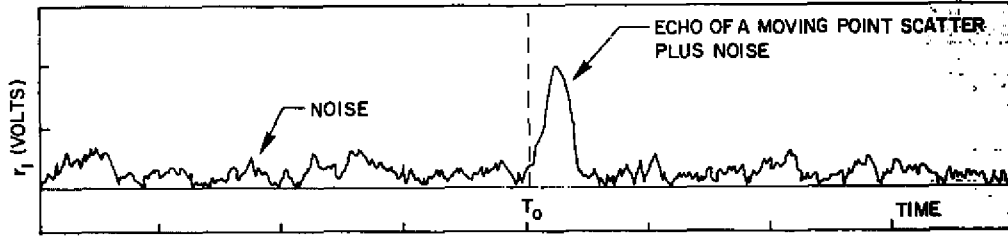
$$y = r_1 - r_2. \tag{2}$$

A typical set of time history recordings of r_1 , r_2 , and y are shown in Fig. 1. Due to target motion the pulse position of r_1 and r_2 are not the same in time; consequently, when y is found, a detectable signal remains. Quantitative results of the system performance are next obtained using the positive residue of (2), which is sufficient due to symmetry.

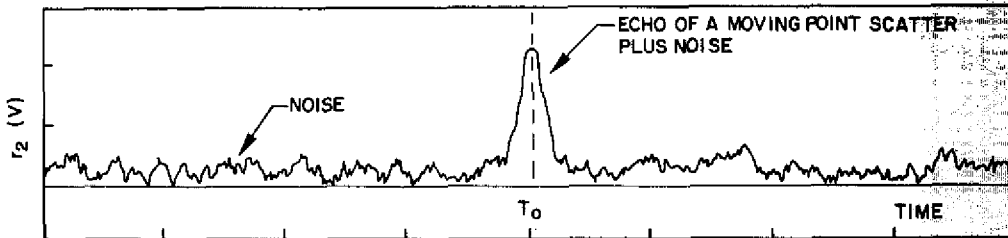
NOISE CHARACTERISTICS AND THRESHOLDS

The probability density of the outputs of the envelope detector r_1 and r_2 under the previous assumptions is a Rayleigh distribution given by

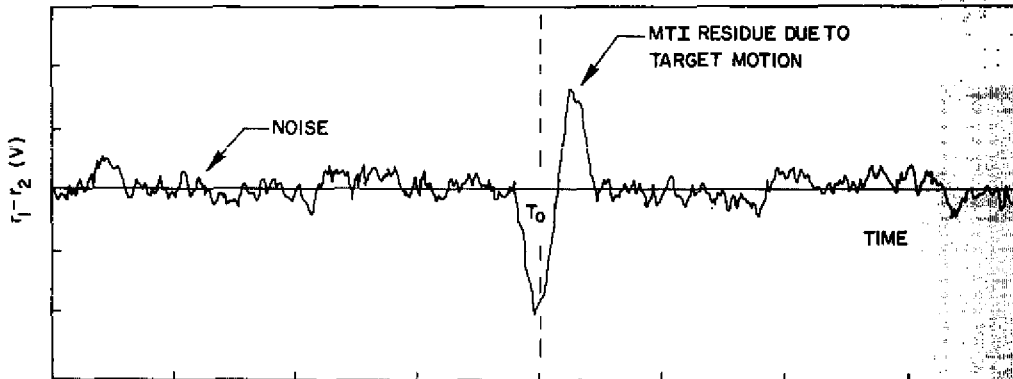
$$p(r_i) = \frac{r_i}{\sigma^2} e^{-r_i^2/2\sigma^2} \quad \text{for } i = 1, 2,$$



(a) Video return r_1 from the first pulse transmission



(b) Video return r_2 from the second pulse transmission



(c) MTI output $y = r_1 - r_2$

Fig. 1 — Typical set of time histories of the video returns of successive pulses and the MTI output of their difference

where r_1 and r_2 are independent. Probability theory states that the probability density of the sum of two independent random variables is the convolution of their two densities and that the difference of two independent random variables is the correlation of their two densities. Consequently the probability density given noise $p(y|N)$ at the output of the MTI is

$$p(y|N) = \int p_{r_2}(r_1 + y)p_{r_1}(r_1) dr_1. \quad (3)$$

When (1) is used in (3), the desired density becomes

$$p(y|N) = \frac{e^{-z^2}}{2\sigma^2} \left[|z| e^{-z^2} + \frac{\sqrt{\pi}}{2} (1 - 2z^2) (1 - \text{erf } |z|) \right],$$

where $z = y/2\sigma$ and

$$\text{erf} = \frac{2}{\sqrt{\pi}} \int_z^\infty e^{-u^2} du.$$

The density has a mean of zero and a standard deviation of 0.926σ , which was found by numerical integration. The density $p(y|N)$ is shown in Fig. 2 for $\sigma = 1$.

Using only the positive residues, the threshold setting γ as a function of probability of false alarm p_{fa} was found numerically by integrating

$$p_{fa} = \int_\gamma^\infty p(y|N) dy,$$

and the results are shown in Fig. 3. The curve is read as follows. The desired probability of false alarm is found on the ordinate and the value of the abscissa is read. This value is multiplied by 2σ to find the threshold γ . The case when signal plus noise is present is next discussed.

SIGNAL-PLUS-NOISE CHARACTERISTICS

The probability density of the output r_i of an envelope detector when the input is a sinusoid in additive Gaussian noise is a Rician distribution given by

$$p(r_i) = \frac{r_i}{\sigma^2} e^{-(r_i^2 + m^2)/2\sigma^2} I_0\left(\frac{r_i m}{\sigma^2}\right) \quad \text{for } i = 1, 2, \quad (4)$$

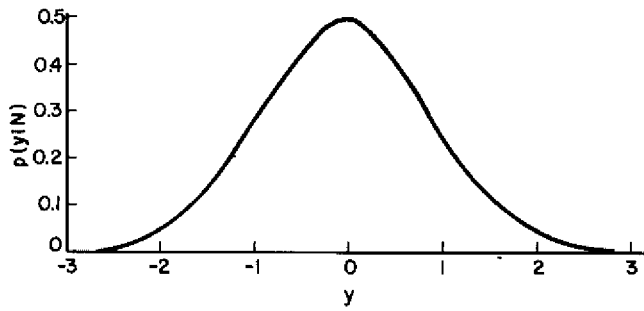


Fig. 2 — Probability density in the case of noise at the output of the MTI with $\sigma = 1$

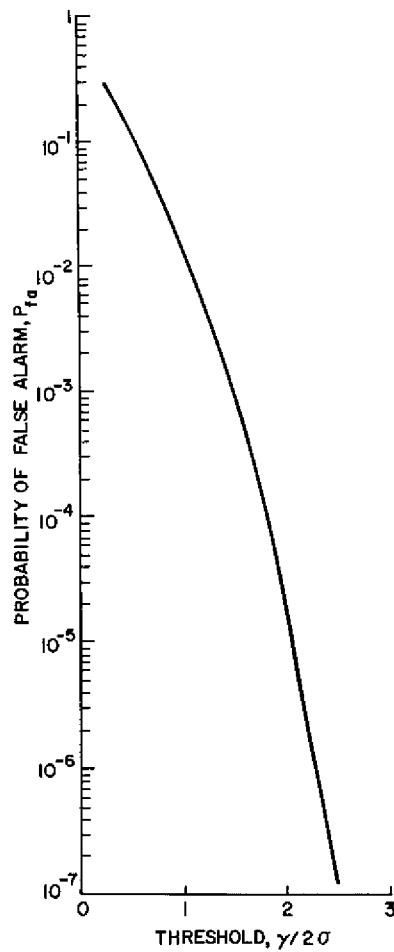


Fig. 3 — Curve relating the threshold γ to the probability of false false alarm

where m is the amplitude of the signal and $I_0(\cdot)$ is the zero-order modified Bessel function. The probability density at the output of the MTI processor is computed similarly as before by correlating the probability densities of r_1 and r_2 given in (4). However closed-form solutions were not obtained. Consequently the results were obtained numerically. The correlation (3) is approximated by the discrete form

$$p(k\Delta) = \Delta \sum_{i=0}^{N-1} p_{r_1}(i\Delta) p_{r_2}[(i+k)\Delta],$$

where $i\Delta = r_1$ and $k\Delta = y$, with Δ being the distance between samples. The probability density of y , given signal plus noise $p(y|S+N)$, is more easily computed using the fast Fourier transform, since correlation corresponds to multiplication in the transform domain. The result is

$$p[y|(S+N)] = IDFT \{DFT^*(p_{r_1}) DFT(p_{r_2})\}, \quad (4)$$

where DFT denotes the discrete Fourier transform, $IDFT$ denotes the inverse discrete Fourier transform and the asterisk denotes the complex conjugate. Examples of the probability densities $p[y|(S+N)]$ are given in Fig. 4. Figure 4a involves subtracting two signals with a signal-to-noise ratio of 13 dB, and Fig. 4b involves subtracting a signal with a signal-to-noise ratio of 13 dB from a signal with noise only. In both cases $\sigma = 1$ and the distributions are Gaussian-like with nearly the same variances. However the means are considerably different. One case corresponds to a point target which is not in motion (equal signal-to-noise ratio on each pulse transmission), and the other case corresponds to a point target in motion such that the signal plus noise is subtracted from noise. Using only the positive residues, the probability of detection is computed by

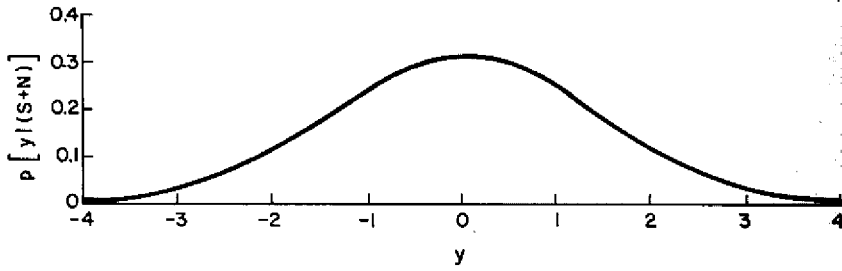
$$p_d = \int_{\gamma}^{\infty} p[y|(S+N)] dy, \quad (5)$$

where the threshold is denoted by γ . A means of setting the false alarm and determining the probability of detection have been obtained for the noncoherent moving-target detector system. The system operating curves for a point scatterer in motion are next obtained.

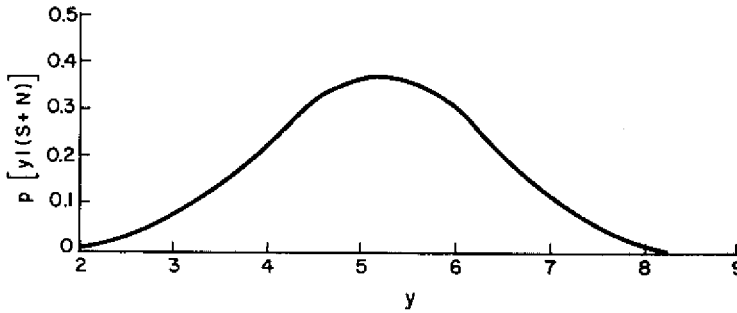
OPERATING CURVES

The result to be obtained is the probability of detection versus point-scatterer velocity for various signal-to-noise ratios and a fixed probability of false alarm. The threshold required for $p_{fa} = 10^{-6}$ is obtained from Fig. 3 and inserted in (5). Time is normalized to the pulse width τ_p . The numerical methods outlined in (4) are used to find $p[y|(S+N)]$, and the probability of detection is found using (5). The results are shown in Fig. 5. The parameter ζ is a normalized velocity. Once the time between pulses T and the pulse width τ_p are chosen, the velocity v can be found by reading ζ from the curve and computing

$$v = \frac{\zeta c \tau_p}{2T},$$



(a) When both r_1 and r_2 have signal-to-noise ratios of 13 dB



(b) When r_1 has a signal-to-noise ratio of 13 dB and r_2 is simply noise

Fig. 4 — Probability density in the case of signal plus noise ($S + N$) at the output of the *MTI* with $\sigma = 1$

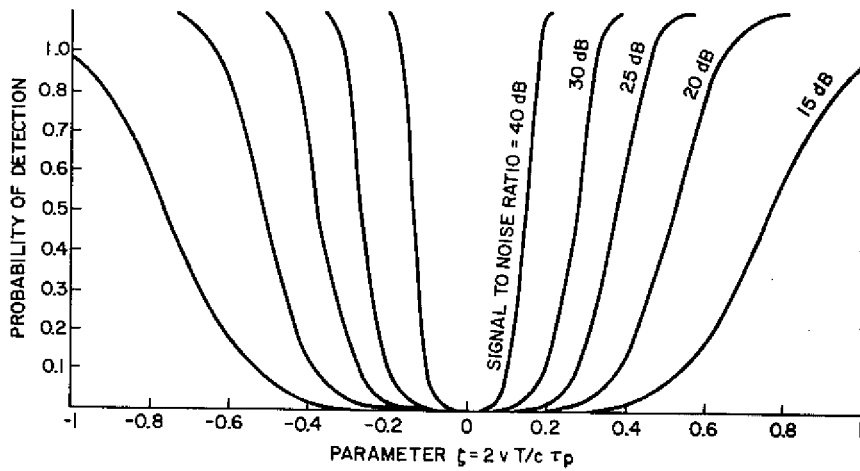


Fig. 5 — *MTI* operating curves: probability of detection versus normalized target velocity for various signal-to-noise ratios and a probability of detector of 10^{-6}

where c is the speed of light. For example a point scatterer moving at 30 m/s and being illuminated with a radar having a 2-n pulse width, using 5-ms time intervals between pulses, and operating with sufficient power to yield a 20-dB signal-to-noise ratio will yield a probability of detection of 0.5.

Low-speed targets have a low probability of detection, and high speed targets have a high probability of detection. This is the desired effect of an *MTI* which is to separate moving targets from nearly stationary clutter. The notch width depends on the signal-to-noise ratio, where the high signal-to-noise ratio targets are not as easily canceled when the two pulses begin to separate in time. This system has no target blind speeds as in coherent *MTI*'s, and the system can be easily designed to have no range ambiguities in most cases.

SUMMARY

A means of discriminating between moving and nonmoving targets using video returns from two successive pulse transmissions of a radar was described. The method relies on the fact that the echoes of moving targets change range and those of slowly moving targets do not. For practical systems this may require fairly short pulses, in the nanosecond class.

The probability density of the noise at the processor output was found in closed form, and the threshold settings for various false-alarm rates were shown. The probability density of signal plus noise was found easily by numerical techniques; consequently the operating characteristics of the system could be computed.

The probability of detection versus target speed for a probability of false alarm of 10^{-6} showed a deep null in detectability for slow-speed targets and a high detectability for other higher speed targets. Consequently moving targets can be distinguished from slow-moving clutter. The system has no blind speeds and can be designed to have no range ambiguities.

ACKNOWLEDGMENT

I thank B. L. Lewis for discussing the problems with me.

REFERENCES

1. M. I. Skolnik, editor, *Radar Handbook*, McGraw-Hill, 1970.
2. M. I. Skolnik, *Introduction to Radar Systems*, McGraw-Hill, 1962.
3. B. L. Lewis and B. H. Cantrell, "Short Pulse Noncoherent MTI," Patent Application Navy Case 60,372, Naval Research Laboratory, Dec. 23, 1975.